CHARACTERIZATION OF STANDARDISED HEAVY RAINFALL PROFILES FOR BARCELONA CITY: CLUSTERING, RAIN AMOUNTS AND INTENSITY PEAKS

Lana X. [(1)], Rodríguez-Solà R.[(1)], Martínez M. D.[(1)], Casas-Castillo M. C.[(1)], Serra C.[(1)], Burgueño A.[(2)]

[(1)] Department of Physics, Universitat Politècnica de Catalunya, Barcelona.

[(2)] Department of Applied Physics – Meteorology, Universitat de Barcelona, Barcelona.

Corresponding author:

Xavier Lana, Department of Physics, Universitat Politècnica de Catalunya, Barcelona. Av. Diagonal 647, 08028 Barcelona, francisco.javier.lana@upc.edu

Short Tittle: Clustering of standardized heavy rainfall profiles.

Abstract

Standardised heavy rainfall profiles may contribute to a best knowledge concerning flash floods, ground erosion and runoff. Taking advantage of the rain rate gauges network of Barcelona city and applying a short integration time of 5-min, the heavy rainfall records with amounts above 25 mm and longer than 60 min have been selected along 15 years, being detected 499 records corresponding to 67 episodes. The amount distribution of these records are analysed at time deciles. By grouping these standardised rainfall profiles according to their similarity by means of the Average Linkage clustering algorithm, 10 clusters are derived, each one of them characterised by different time evolution of rainfall. The representative standardised rainfall profiles for every one of the clusters, together with maximum 5-min rain amounts and rainfall amounts characterizing them, permit to distinguish rainfall patterns. In addition, the extreme heavy rainfalls which may lead to flash floods are identified, as also their respective synoptic situations. In short, this analysis offers a description of heavy rainfall patterns in Barcelona city, complementing previous papers on the normalized intensity curves and 5-min intensity return periods. These heavy rainfall analyses would be very useful when designing drainage and sewerage systems in urban areas as Barcelona, where flash floods may be expected due to episodes of notable rainfall amount and intensity. The imperviousness density of the soil and an appropriate sewerage structure should be adapted to mitigate the effects of these copious and intense episodes.

Key-words: 5-min rain amounts, rain rate gauges network, standardised rainfall profile, heavy rainfalls, average linkage clustering algorithm, Barcelona urban area.

1.INTRODUCTION

Urban rainstorms, sometimes characterised by copious amounts in short time intervals with outstanding high intensities, may produce flash floods exceeding urban drainage system capacity. Consequently, several heavy rainfall patterns (lengths, rainfall amounts and rainfall intensity peaks) should be analysed to prevent possible urban flash floods or mitigate their effects (e.g. Pilgrim and Cordery, 1975; Keifer and Chu, 1997; Arnaud et al., 2002; Hamidreza et al., 2010). Modifications on precipitation extremes due to climatic change should also be taken into consideration in urban drainage designs (e.g. Willems, 2013; Simonovic et al., 2016; Fadhel et al., 2017; Hosseinzadehtalaei et al., 2018; Acquaotta et al., 2018).

Among the different ways for analysing the time distribution of storm rainfall from a set of rain rate gauges covering a certain domain, the Huff curves (Huff, 1967, 1970, 1990; Bonta, 2004) have been worldwide applied to different regions (Al-Rawas and Valeo, 2009; Azli and Rao A. R., 2010; Ghasemi et al., 2014; Nojumuddin et al., 2015; Dolšak et al., 2016) as also to cities (Chen et al, 2015; Pan et al., 2017) or single rain rate gauges (Burgueño et al., 1994; Bonta and Shahalam, 2001; Back, 2011). The Huff curve, known as standardized rainfall profile or hyetograph, has also permitted to describe the within-storm temporal pattern by comparing areas under this curve for the four time quartiles (Terranova and Laquinta, 2011; Terranova and Gariano, 2014). In urban domains, the spatial and temporal variability of rainfall fields may be also obtained from the attenuation of microwave signals over the city by means of radars (Emmanuel et al., 2012; Wright et al., 2012) or by mobile phone infrastructures (Cuccoli et al., 2013). As known, the urban heat island (UHI) may lead to an increase of extreme precipitations collected over or downwind of cities, as a result of the small scale surface convergence induced by the UHI (Kishtawal et al., 2010; Schmid and Niyogi., 2013; Han et al., 2014). For coastal cities, in summer, the humid air incoming due to sea breeze usually intensify this phenomenon (Ganeshan et al., 2013; Kusaka et al., 2014; Han et al., 2015; Argüeso et al., 2016).

In here, heavy rainfall recorded in a network of rain rate gauges spread over Barcelona city (NE Spain) along 15 years is the object of analysis. The rainfall regime in Barcelona has an annual average close to 620 mm/year and a standard deviation of 150 mm/year, according to Fabra Observatory (Barcelona) records for the period 1917–2009. As well known, heavy rainfalls are characteristic of Mediterranean climate. For instance, close to 100 daily episodes above 60 mm/day have been recorded at Fabra Observatory along the indicated period. More details concerning the Fabra Observatory rainfall regime at annual, monthly, and daily scales can be found in Burgueño et al. (2004) and Lana et al. (2005), among others.

The long dry spells are another characteristic of the Barcelona rainfall regime (Lana et al., 2006, 2017), especially in summer. These dry spells may be sometimes interrupted at the end of August and along September, October or November by relatively short, but intense, rainfall episodes. Whereas moderate and

intense storms usually happen at the end of August and along September due to air mass convective phenomena, eastern advections, sometimes with notable rain amounts, usually occur along October and November. By one hand, these rainfall episodes contribute to mitigate the effects of droughts on the environment, especially when the rainfall amounts have been small in the spring season and this deficit is hardly compensated along the summer season. On the other hand, high rainfall intensities, accompanied by copious rainfall, may generate flash floods. An illustrative example of these heavy rainfall episodes could be that corresponding to September 6, 2018, when a convective process produced a copious stormy rainfall over Barcelona metropolitan area, being exceeded the urban drainage system. According to the *Servei Meteorològic de Catalunya*, SMC, a notable amount of 110.0 mm (15-20% of the average annual amount) was recorded close to Barcelona city along approximately 3 h. Additionally, a rain gauge of the SMC in Barcelona downtown (Barcelona-El Raval) recorded a very high amount of 58.7 mm in 30-min, with a maximum intensity of 4.9 mm/1-min. The total amount recorded in 60 min was 83.3 mm, which corresponds to a return period of 70 years in agreement with Casas et al. (2004).

Some years ago the incidence of copious rainfall storms with high rainfall intensity in Barcelona urban area was studied by means of the Intensity-Duration-Frequency (IDF) curves (Redaño et al., 1986; Raso et al., 1995; Casas et al, 2004, 2010), the expected maximum rainfall for a length and a given return period being derived. These curves were of application in different municipal sewerage plans in Barcelona. The probable maximum precipitation in Barcelona was also estimated (Casas et al., 2011). At the present study, previous analyses on the normalised intensity curves and return period curves at 5-min scale for Barcelona urban network (Lana et al, 2018a,b) are complemented by considering standardised profiles for heavy rainfall across the city from 5-min rain amounts. Profiles corresponding to the most copious rain amounts and heaviest rainfall intensities, which may contribute to flash floods, are analysed in detail. Taking advantage of the 23 Barcelona tipping bucket rain rate gauges network (Figure 1), the different profiles of heavy rainfall are distinguished and examined.

The contents of the paper are organised as follows. Section 2 (Database) briefly describes the instrumental characteristics of the urban network, its spatial distribution and thresholds considered for amounts and lengths. These thresholds have been chosen with the aim of selecting heavy rainfalls, which may produce runoff problems or possible flash floods. Preliminary statistics are also given. Section 3 briefly describes the average linkage, AL, clustering algorithm and the similarity index, L_{ij}, which permit an objective classification of rainfall profiles in different homogeneous clusters. Section 4 details the properties of the clusters obtained and analyses the extreme heavy rainfall, including their atmospheric synoptic situations. Section 5 (Conclusions) summarises the most relevant results and points out where flash floods are likely to happen, paying attention to the spatial distribution of the gauges.

2. DATABASE

2.1 DATABASE DETAILS

A large pluviometric dataset for the urban area of Barcelona (approximately 100 km^2) has been in operation by means of the CLABSA pluviometric network from September 1994 until November 2009 (Figure 1, Table 1). This network has consisted of 23 tipping bucket rain rate gauges, brand Geónica S. A., with a 400-cm^2 collector funnel and a rain rate resolution of 0.1 mm / 5-min (Casas et al. 2010; Rodríguez et al. 2014). The rainfall intensity has been recorded by tipping bucket gauges, with an integration time depending on the rain rate. To permit a common and uniform integration time, the measured intensities have been converted to amounts recorded in 5-min intervals. The topography of the urban area (Figure 1) is characterised by a low hill (150 m a.s.l.) close to the harbour, with a steep slope faced to the coast, and a relatively flat area extending from the coast line to the foot of the littoral chain, which achieves altitudes up to 500 m a.s.l. The elevation range of the gauges extends from close to the shore line up to 415 m a.s.l. (Fabra Observatory).

With respect to the selection of a specific record length for every gauge, two considerations (Lana et al, 2018a, b) are taken into account:

- A record starts for a gauge when a 5-min amount above or equal to 0.1 mm/5-min is detected, provided that this threshold has not been exceeded at least 1 h before.
- A record finishes for a gauge when a waiting time longer than 1 h is detected after the last 5-min amount above or equal to 0.1 mm/5-min.

Then, records for a gauge can include several 5-min intervals with amounts below the rain rate resolution, but shorter than 1 h. These intervals could be considered as rainfall intermittences within the same rainfall record and they could be sometimes a relevant pattern of a 5-min intensity profile.

The selection of rain amounts and rainfall intensities overpassing urban drainage systems and causing flash floods is quite difficult bearing in mind specific ground characteristics (imperviousness density) and drainage systems. In agreement with the *Agencia Española de Meteorología*, AEMET[(a)] exceedances of 60, 100 and 180 mm along 12 h could generate floods in the Mediterranean coast close to Barcelona metropolitan area with notable, high and very high probability respectively. Alternatively, rainfall intensities above 20, 40 and 90 mm in 1 h could produce similar consequences. Other slightly different amount thresholds are suggested by the SMC[(b)] (100 mm and 200 mm in 24 h), with rainfall intensities above 20 and 40 mm in 30 min being able to cause floods.

[(a)] www.aemet.es/documentos/es/eltiempo/prediccion/avisos/plan_meteoalerta/plan_meteoalerta.pdf

[(b)] www.meteo.cat/wpweb/divulgacio/la-prediccio-meteorologica/avisos-smp/

Due to these different criteria to establish the amount and length to be exceeded with the risk of flash flood, thresholds of 25 mm (Huff, 1967) and 60 min have been finally chosen for Barcelona city. Consequently, all the selected rainfall records for Barcelona satisfy three constraints. First, rainfall amounts have return periods longer than or equal to 1 year (Casas et al. 2010, 2011). Second, only rainfall records with rain amounts above or equal to 25 mm are chosen assuming that smaller amounts should not produce flash floods. And third, lengths of rainfall episodes are longer or equal to 60 min.

In agreement with the first constraint, 188 heavy rainfall episodes have been selected for the whole network. When considering the set of gauges and after discarding specific records not accomplishing the second and third constraints, 528 5-min rain amount records are selected. Finally, this number is reduced taking into account some temporal lacks of data due to technical problems on gauges. In short, a database of 499 5-min rain amount records corresponding to 67 episodes has been obtained. Figure 2a shows all the rainfall records according their amount and length, where dashed lines represent the 25 mm and 60 min thresholds and the solid line depicts the increasing tendency of the rainfall amount R with the episode length L. Figures 2b and 2c show the rain amount and maximum 5-min rain amount for the heavy rain records along the calendar days, being quite evident that the highest values of both variables appear from July to beginning of December and from August to November respectively. Similarly, Figure 2d shows the average rainfall intensity (mm/min) along the calendar days, with the highest values detected within the same months as Figure 2c.

2.2 PRELIMINARY STATISTICS

Several preliminary statistics of the heavy rainfall records for every gauge are summarised in Table 1. The range of variation of the average amount <R> is relatively small (43.6 - 57.7 mm), but the corresponding standard deviation range is wider (15.1 – 30.4 mm), thus pointing to probable differences on the spatial distribution of the rainfall. The average length <L> varies within a relatively short interval (339 – 582 min), but the wide standard deviation range (240 – 427 min) suggests again notable differences on the rainfall spatial distribution. This possibility could be confirmed by observing the ranges of average and standard deviations of maximum 5-min rain amount, I_{max}. Whereas only for gauges 4, 11 and 20 the average I_{max} exceed 6.0 mm/5-min, for the whole set of gauges the standard deviations are within a short range from 2.6 to 3.6 mm/5-min. The hypothesis of a heterogeneous spatial distribution of rainfall is reinforced by revising the largest I_{max}, I_M, for every gauge. The range is wide (9.0 – 19.6 mm/5-min), gauges 5, 6 and 11 having values of I_M above or equal to 14.0 mm/5-min. It is also worth mentioning that the rainfall records with the largest I_{max} usually have notable amounts. Once again some examples could be that corresponding to gauges 5, 6 and 11, with $R(I_M)$ above 58 mm. Other questions have to be also considered. For instance, I_M of gauge 23 (11.3 mm/5-min) is relatively low, while the $R(I_M)$ collected was very high (94.2 mm). In short,

for some gauges, copious amounts are concentrated on short time intervals, sometimes this fact giving rise to flash floods. Nevertheless, this behaviour of the rainfall regime cannot be assumed for the whole network given that the ratio of maximum 5-min rain amount with respect to the record amount (Table 1) varies from 12.0% (gauge 23) to 47.2% (gauge 13), this fact emphasising the spatial heterogeneity of the heavy rainfall.

In agreement with I_M and its ratio $R(I_M)$ relative to the respective R, heavy rainfalls feasible to result in flash floods would appear along July (one gauge), August (three gauges), September (13 gauges), October (five gauges) and November (one gauge). Because most of extreme episodes have been recorded in September and October, air mass convective phenomena (summer) and eastern advections (autumn) would be the atmospheric mechanisms leading to flash floods. If the possibility of flash floods was restricted to records with the highest I_{max}, R and their ratio, gauges 5, 6, 10 and 11 would be considered as those with more likely flash floods, with three rainfall episodes in September and another at the end of August.

Table 2 gives three examples of episodes with heavy rain recorded by the network. These three episodes occurred in September and at the end of August and include some records with I_{max} up to 19.6 mm/5-min, with notable amounts up to 40.5 mm (gauge 10, third episode), 67.4 mm (gauge 5, second episode) and 91.9 mm (gauge 6, first episode). For instance, it is noticeable that for the episode of 09/14/1999 gauge 5 recorded approximately 25% of the total rain amount in 5-min, while the rest of rainfall was collected along 70 min. A similar behaviour is detected for gauges 6 and 10, without any homogeneous spatial distribution of rainfall. I_{max} values are also very varied, ranging from 2.4 to 15.5 mm /5-min. For the episode of 09/21/1995, R range from 6.1 to 91.9 mm, with a wide range of I_{max} (from 0.6 to 19.6 mm/5-min). As a summary, the heterogeneous spatial distribution of heavy rainfall is again quite evident. A possible explanation to this spatial heterogeneity for a relatively small area (close to 100 km^2) could be the convective mechanisms implied in heavy rainfalls, due to air masses storms or to eastern advections, very common the first at the end of August and the second along September and October.

3. METHODOLOGY

3.1 DATA ARRENGEMENT FOR CLUSTERING

For a useful application of the clustering process it is convenient to create the standardised rainfall profile for every record from the 5-min rain amounts recorded along the time. First, every record length is normalised and divided in time deciles. Then, the wide range of record lengths does not condition clusters composition. And second, every 5-min rain amount in a record is accumulated in its corresponding time decile, being the respective rain amounts normalised. In this way, rainfall records with similar standardised rainfall profiles are ready to be grouped by means of the AL clustering algorithm. In short, the clustering is not achieved based on pure lengths and rain amounts but on standardised rainfall profiles computed for every 5-min rain amounts record.

3.2 AVERAGE LINKAGE ALGORITHM

The AL clustering algorithm is applied to the set of standardised rainfall profiles to obtain several clusters, everyone with different rainfall patterns. The AL clustering algorithm process (Kalkstein et al., 1987; Huth et al., 1993; Lana and Fernández-Mills, 1994; Živković, 1995) is based on the L_{ij} parameter, which is defined as

$$L_{ij} = {}^{W_i}/_{N_i} + {}^{W_j}/_{N_j} + D_{ij}^2 \quad (1)$$

with N_i and N_j the number of elements belonging to clusters i and j, W_i and W_j the within-group sum of squares and D_{ij} the Euclidean distances between centroids of clusters i and j. The sum of squares and Euclidean distances are computed taking the amount percentages of time deciles as coordinates of the different elements. At each step of the algorithm, L_{ij} measures the disparity among all possible cluster pairs, thus choosing the fusion linked to its minimum value. In the first step of the algorithm every rainfall record (normalised 5-min rain amounts) is a cluster. After that, for every step of the algorithm, two clusters associated with a minimum of L_{ij} are merged in a new single cluster. The evolution of the minimum L_{ij} for every step of the AL procedure permits to detect when two notably dissimilar clusters are put together in a same cluster. When this situation is found (indicated by a sharp increase on the L_{ij} evolution), the previous configuration of clusters is chosen as the optimal classification of the amount percentages for the different time deciles.

Third, after having chosen the optimal number and configuration of clusters, the averaged amount percentage for every time decile is computed for every cluster, with these averaged percentages being the profiles describing the different rainfall patterns. The degree of irregularity, φ, for every profile is quantified assuming that a theoretical uniform rainfall profile should have equal amount percentages, $P_0 = 0.1$ (10% of the whole recorded rainfall), for the ten time deciles. In other words,

$$\varphi = \left\{\frac{1}{10}\sum_{i=1}^{10}(P_i - P_0)^2\right\}^{1/2} \quad (2)$$

with P_i the relative contribution of the ith time decile precipitation to the whole rainfall amount. In this way, a larger irregularity corresponds to a larger φ value.

4. RESULTS

4.1 CLUSTERING OF PROFILES

The application of the AL clustering algorithm to the selected 5-min rain amount records, characterised by the amount percentages for each time decile, permits to classify them in 10 clusters. The number of possible clusters is established by following the evolution of L_{ij} every time two clusters are merged (Figure 3). Up to a structure of 10 clusters the increase of L_{ij} is almost monotonous. However, when a reduction to 9 clusters is attempted, a sharp increase of L_{ij} is observed, suggesting that the two clusters to be grouped are notably dissimilar and the clustering process should finish with the configuration of 10 clusters.

The most relevant characteristics of the 10 clusters are summarised in Table 3. Whereas clusters 1, 4 and 5 include a great ratio of the total number of records, clusters 2, 3, 6, 7, 8, 9 and 10 comprise only a few records, all of them presenting some singularities in their profiles. Clusters 1 and 4 are characterised by the highest average R and the maximum I_{max}. Whereas clusters 1, 4 and 5 are generated by records belonging to a high number of episodes (41, 32 and 15 respectively), the remaining clusters contain a low number of records associated with only a few episodes (from 1 to 9 depending on the cluster).

The mean rainfall profiles for every cluster, with average rain amount percentages along the time deciles, are shown in Figure 4, where the dashed line represents the uniform distribution of rainfall (the same percentage for every one of the time deciles). Cluster 1, including the largest number of records (225), has a profile characterised by percentages (<30%) relatively close to the uniform distribution of rainfall along the record. Cluster 2 consists on a low number of records (4) and is characterised by profiles beginning with moderate percentages (<40%) that diminish slowly towards the end of the record. Cluster 4 is another group with a high number of records (178), where the maximum percentage, not exactly at the beginning of the record, keeps below 40% and the percentages also reduce their value towards the end of the record. The rest of clusters are characterised by profiles with notable percentages reached for only one or two time deciles, sometimes up to 85% of the whole recorded rainfall (cluster 10). As a general rule, the number of records assigned to every one of these clusters is low, excepting cluster 5. For this cluster the highest percentage for a time decile (≈ 50%) is usually found towards the end of the record. Taking advantage of the obtained 10 cluster profiles (Figure 4), the departure of every cluster profile with respect to uniform rainfall percentages along time deciles is quantified by the degree of irregularity φ (Equation 2) and their values are given in Table 4. Clusters 1 and 4 have the most uniform rainfall profiles, with φ values below 10. On the contrary, the rainfall is highly concentrated in one or two time deciles for clusters 3, 6, 7, 9 and 10, with values of φ exceeding or close to 20. Records assigned to these clusters could lead to flash floods due to the concentration of a notable ratio of the rainfall in a low number of time deciles. Nevertheless, the

records belonging to these clusters do not appear within the extreme heavy rainfalls, which are analysed in the next Section 4.2. Consequently, a high degree of irregularity φ would not be a sign of extreme heavy rainfall, but only a parameter to quantify the difference with respect to uniform rainfall percentages along time deciles.

Figure 5 shows 5-min rain amount records for four gauges pertaining to clusters 1, 3, 4 and 5. These episodes are selected on account of their remarkable, sometimes copious, R and high I_{max}, thus being prone to cause flash floods. The first record pertaining to cluster 1 is characterised by an amount of 58.2 mm and I_{max} of 14.0 mm / 5-min, which represents close to 25% of the total amount. Most of rainfall is recorded along approximately 25 min, in the middle of the record. The second record (cluster 3) has a lower amount and very similar I_{max} to the previous record. In this case, the I_{max} occurs at the beginning of the episode, contributing to close to 20% of the total amount. The third record (cluster 4) has a very high amount (91.9 mm) and I_{max} (19.6 mm/ 5-min). It is also relevant that along 40 min the rainfall amount is a high percentage of the cumulative total of 91.9 mm. The fourth record (cluster 5) depicts some similar characteristics to those observed in the second example with respect to R and I_{max}. Rainfall intermittences are clearly observed and the I_{max} is shifted towards the end of the record.

4.2 EXTREME HEAVY RAINFALLS

The selection of records most likely to lead to flash floods is proposed to be based on the largest I_{max}, R/L and R exceeding their respective 95% percentiles (7.9 mm/5-min, 0.22 mm/min and 55.2 mm). The rainfalls hypothetically causing flash floods are chosen if the three exceedances are accomplished at the same time, these exceptional records being termed extreme heavy rainfalls. Figure 6 shows the roughly linear increasing trend of I_{max} on R/L for the whole set of records, including the extreme heavy rainfalls. Assuming these three 95% percentiles thresholds, 29 records of eight rainfall episodes would be associated with very likely flash floods due to copious rainfall with high I_{max}, notable R/L and copious R. Certainly, these eight exceptional episodes caused flash flood damages affecting, among others, public transport services and basements, with some deceases, as proved by local newspapers and scientific researches (Barrera et al., 2006; Llasat et al., 2014).

Table 5 summarises the main characteristics of these extreme heavy rainfalls, with I_{max} ranging from 7.9 to 19.6 mm/5-min, R from 55.1 to 136.5 mm and R/L from 0.23 to 0.82 mm/min. It is also remarkable the ratio (percentage) of I_{max} with respect to the corresponding amount R of the record, which ranges from a small 6.6% to a notable 24.1%. Table 5 includes the corresponding cluster for the selected records. 16 extreme records correspond to cluster 1, 11 to cluster 4 and two to cluster 5. In consequence, 27 records (clusters 1 and 4) have moderate irregularity of percentages assigned to every time decile (a maximum of 25-30% for

one or two deciles). The other two records (cluster 5) have a notable irregular rainfall profile, with close to 50% of R assigned to a single time decile. Consequently, in most of the extreme records, R and R/L would be more relevant than I_{max}. Only for the two cases belonging to cluster 5, in spite of their relatively moderate R, flash flood risk might exist, because I_{max} would represent an outstanding percentage of R, as shows for instance the seventh time decile of the profile in Figure 4. It is worth mentioning that for 13 out of 29 records I_{max}, R and R/L exceed 13.1 mm/5-min, 106.6 mm and 0.50 mm/min, which are thresholds given by the averaged values plus one standard deviation for every variable. It is also noticeable that gauges 1, 8, 9, 12, 13 and 18 have not recorded any extreme heavy rainfall. Consequently, these gauges would pertain to areas of Barcelona with low flash flood risk. Conversely, only gauges 5, 6 and 11 have very high values notably exceeding 95% percentiles for, at least, two out of the three variables characterising flash flood risk. It should be underlined that the emplacement of these three gauges is very close to places where maximum 5-min amounts for return periods of 10 and 25 year were detected by Lana et al. (2018b).

Revision of surface and 500 hPa meteorological maps (http://www.wetterzentrale.de) for the eight episodes producing extreme heavy rainfalls (Table 5) indicates that their synoptic situations have similar patterns. By one hand, small and very weak surface pressure gradients with null or very light eastern advection over the Iberian Peninsula; on the other hand, a trough at 500 hPa, with Barcelona in its onward side, with flux of northern cold winds at the corresponding altitudes. These facts, together with the vicinity to the warm Mediterranean Sea may develop convective activity producing heavy thunderstorms. Certainly, other questions, besides to meteorological factors, such as drainage system design, ground runoff or impervious surfaces (as concrete or asphalt), will finally determine whether these extreme heavy rainfalls result in flash floods and their effects. As the extreme heavy rainfalls (Table 5) correspond to July (2), August (1), September (4) and October (1), it should be assumed that flash floods episodes in Barcelona are more likely in summer and the beginning of autumn.

5. CONCLUSIONS

The 5-min rain amount measurements in 23 gauges across Barcelona for 15 years have permitted to verify the heterogeneous spatial distribution of heavy rainfalls and determine several characteristics of copious rainfalls related to flash flood episodes. The AL clustering algorithm has classified 499 records of heavy rainfall in 10 clusters. Different rainfall records of a same gauge can appear in different clusters. In this way, the AL algorithm does not classify gauges or episodes, but detects standardised rainfall profiles with very similar patterns. Every one of the mentioned clusters is characterised by a different value of the degree of irregularity, being confirmed the different rainfall profiles. Whereas a good ratio of rainfall records are characterised by a notable regularity (clusters 1 and 4), a small number of rain records have strong (clusters 3, 5, 6, 7, 9 and 10) and moderate (clusters 2 and 8) irregularities. It is also worth mentioning that the time decile with the highest percentage of rainfall amount is expected at the beginning, the middle or the end of the rainfall episode, depending on the cluster.

With respect to the extreme heavy rainfalls associated with flash flood episodes, these are specially detected close to emplacements of gauges 5, 6, and 11, in agreement with previous analyses of return period values of 5-min intensity for 10 and 25 years. Additionally, these records have been assigned by the AL algorithm only to clusters 1, 4, and 5. These extreme heavy rainfalls have been detected since middle summer to the beginning of autumn. In agreement with these seasons and typical characteristics of the western Mediterranean climate, extreme heavy rainfalls would be generated by convective phenomena producing copious amounts with high rainfall intensities. The forecasting of these episodes is not so evident from surface and 500 hPa charts, taking into account that surface pressure gradient uses to be almost null in these cases.

The results obtained in this paper may be also a complement to previous analyses made to design drainage and sewerage systems to prevent or mitigate flash floods effects generated by copious rainfall episodes with short intervals of high intensity. From this point of view, it would be relevant to remember that just some gauges are associated with extreme rain amounts and the highest rain intensities. Consequently, this spatial heterogeneity of flash flood risks, together with imperviousness density and the topography of the urban domain, should be taken into account for improving drainage and sewerage systems. Facilitating the infiltration of rainfall water in the ground would mitigate runoff, sometimes preventing or reducing the saturation of a sewer network. Additionally, the mitigation of urban heat island phenomenon could not be discarded when a not negligible amount of rain water was absorbed by a porous ground.

REFERENCES

Acquaotta F., Faccini F., Fratianni S., Paliaga G., Sacchini A., Vilímek V. (2018) Increased flash flooding in Genoa Metropolitan Area: a combination of climate changes and soil consumption?. Meteorology and Atmospheric Physics, 131, 1099-1110

Al-Rawas G.A., Valeo C. (2009) Characteristics of rainstorm temporal distributions in arid mountainous and coastal regions. Journal of Hydrology, 376, 318–326.

Azli M., Ramachandra Rao A. (2010) Development of Huff curves for Peninsular Malaysia, Journal of Hydrology, 388, 77–84.

Argüeso D., Di Luca A., Evans J.P. (2016) Precipitation over urban areas in the western Maritime Continent using a convection permitting model. Climate Dynamics, 47, 1143–1159.

Arnaud P., Bouvier C., Cisneros L., Dominguez R. (2002) Influence of rainfall spatial variability on flood prediction. Journal of Hydrology, 260(1), 216-230.

Back Á. J. (2011) Time distribution of heavy rainfall events in Urussanga, Santa Catarina State, Brazil. Acta Scientiarum. Agronomy. Maringá, 33, 583-588.

Barrera A., Llasat M.C., Barriendos M. (2006) Estimation of extreme flash flood evolution in Barcelona County from 1351 to 2005. Natural Hazards and Earth System Sciences, 6, 505-518.

Bonta J.V., Shahalam A. (2001) Cumulative storm rainfall distributions: comparison of Huff curves. Journal Hydrology New Zealand, 42, 65-74.

Bonta J. V. (2004) Development and utility of Huff curves for disaggregating precipitation amounts. Applied Engineering in Agriculture, 20, 641−653

Burgueño A., Codina B., Redaño A., Lorente J. (1994) Basic statistical characteristics of hourly rainfall amounts in Barcelona (Spain). Theoretical and Applied Climatology, 49, 175-181.

Burgueño A., Serra C., Lana X. (2004) Monthly and annual statistical distributions of the daily rainfall at the Fabra Observatory (Barcelona, NE Spain) for the years 1917 –1999. Theoretical and Applied Climatology, 77, 57 –75.

Casas M.C., Codina B., Redaño A., Lorente J. (2004) A methodology to classify extreme rainfall events in the western Mediterranean area. Theoretical and Applied Climatology, 77, 139 –150.

Casas M.C., Rodríguez R., Redaño A. (2010) Analysis of extreme rainfall in Barcelona using a microscale rain gauge network. Meteorological Applications, 17,117–123.

Casas M.C., Rodríguez R., Prohom M., Gázquez A., Redaño A. (2011) Estimation of the probable maximum precipitation in Barcelona (Spain). International Journal of Climatology, 31, 1322–1327.

Chen Z., Yin L., Chen X., Wei S., Zhu Z. (2015) Research on the characteristics of urban rainstorm pattern in the humid area of Southern China: a case study of Guangzhou City. International Journal of Climatology, 35, 4370-4386.

Cuccoli L., Baldini L., Facheris L., Gori S., Gorgucci E. (2013) Tomography applied to radiobase network for real time estimation of the rainfall rate fields. Atmospheric Research, 119, 62–69.

Dolšak D., Bezak N., Šraj M. (2016) Temporal characteristics of rainfall events under three climate types in Slovenia. Journal of Hydrology, 541, 1395–1405.

Emmanuel I., Andrieu H., Leblois E., Flahaut B. (2012) Temporal and spatial variability of rainfall at the urban hydrological scale. Journal of Hydrology, 430–431, 162–172.

Fadhel S., Rico-Ramirez M. A., Han D. (2017) Uncertainty of Intensity–Duration–Frequency (IDF) curves due to varied climate baseline periods. Journal of Hydrology, 547, 600–612.

Ganeshan M., Murtugudde R., Imhoff M.L. (2013) A multi-city analysis of the UHI-influence on warm season rainfall. Urban Climate, 6, 1–23.

Ghasemi A., Mirzaei S., Mirzaei Y., Raoof M., Moradnezhadi M. (2014) Effect of Climate on Temporal Distribution Pattern of Rainfall andComparing With Each other ANF Known Patterns Case Study: Ardebil Province – Iran. Bulletin of Environment, Pharmacology and Life Sciences, 3, 118-125.

Hamidreza M.G., Hasan A., Mohammad J. (2010). Study of the temporal distribution pattern of rainfall effect on runoff and sediment generation using rain simulator. World Applied Sciences Journal, 11, 64- 69.

Han J.Y., Baik J.J., Lee H. (2014). Urban Impacts on Precipitation. Asia-Pacific Journal of Atmospheric Sciences, 50, 17-30, DOI:10.1007/s13143-014-0016-7.

Han L., Xu Y., Pan G., Deng X., Hu C., Xu H., Shi H.(2015) Changing properties of precipitation extremes in the urban areas, Yangtze River Delta, China, during 1957–2013 Natural Hazards, 79, 437–454. DOI 10.1007/s11069-015-1850-3.

Hosseinzadehtalaei P., Tabari H., Willems P. (2018) Precipitation intensity–duration–frequency curves for central Belgium with an ensemble of EURO-CORDEX simulations, and associated uncertainties. Atmospheric Research, 200, 1-12.

Huff F.A. (1967). Time distribution of rainfall in heavy storms. Water Resources Research, 3, 1007-1019.

Huff F.A. (1970). Time distribution characteristics of rainfall rates. Water Resources Research, 6, 447-454.

Huff F.A. (1990) Time distributions of heavy rain storms in Illinois. Illinois State Water Survey, Champaign, Circular, 173 pp.

Huth, R., Nemesova, I., Klimperová, N. (1993). Weather categorization based on the average linkage clustering technique: An application to European mid-latitudes. International Journal of Climatology, 13, 817-835. doi.org/10.1002/joc.3370130802.

Kalkstein L.S., Tang G., Skindlov J.A. (1987). An evaluation of three clustering procedures for use in synoptic climatological classifications. Journal of Climate and Applied Meteorology, 26, 717–730.

Keifer C.J., Chu H.H. (1997) Synthetic storm pattern for drainage design. *Journal of the Hydraulics Division*, 83, 1-25.

Kishtawal C.M., Niyogi D., Tewari M., Pielke R.A., Marshall Shepherd J. (2010) Urbanization signature in the observed heavy rainfall climatology over India. International Journal of Climatology, 30, 1908–1916.

Kusaka H., Nawata K., Suzuki-Parker A. , Takane Y. , Furuhashi N. (2014) Mechanism of Precipitation Increase with Urbanization in Tokyo as Revealed by Ensemble Climate Simulations. Journal of Applied Meteorology and Climatology, 53, 824-839.

Lana X., Fernández-Mills G. (1994) Minimum sample size for synoptic weather type classification. Application to winter period data recorded in the Catalan coast (NE–Spain). International Journal of Climatology, 14, 1051–1060.

Lana X., Martínez M.D., Serra C., Burgueño A. (2005) Periodicities and irregularities of indices describing the daily pluviometric regime of the Fabra Observatory (NE Spain) for the years 1917-1999. Theoretical and Applied Climatology, 82, 183-198.

Lana X., Martínez M.D., Burgueño A., Serra C., Martín-Vide J., Gómez, L. (2006) Distribution of long dry spells in the Iberian Peninsula, years 1951-1990. International Journal of Climatology, 26, 1992-2021.

Lana X., Burgueño A., Serra C., Martínez M.D. (2017) Multifractality and autoregressive processes of dry spell lengths in Europe: an approach to their complexity and predictability. Theoretical and Applied Climatology, 127, 285-303. doi 10.1007/s00704-015-1638-0.

Lana X., Serra C., Casas-Castillo M.C., Rodríguez-Solà R., Redaño A., Burgueño A. (2018a) Rainfall intensity patterns derived from the urban network of Barcelona (NE Spain). Theoretical and Applied Climatology, 133, 385-403. doi 10.1007/s00704-017-2193-7.

Lana X., Casas-Castillo M.C., Serra C., Rodríguez-Solà R., Redaño A., Burgueño A., Martínez M.D. (2018b) Return period curves for extreme 5-min rainfall amounts at the Barcelona urban network. Theoretical and Applied Climatology. doi 10.1007/s00704-018-2434-4.

Llasat M.C., Marcos R., Llasat-Botija M., Gilabert J., Turco M., Quintana-Seguí P. (2014) Flash flood evolution in North-Western Mediterranean. Atmospheric Research, 149, 230-243.

Nojumuddin N.S., Yusof F., Yusop Z. (2015) Identification of Rainfall Patterns in Johor. Applied Mathematical Sciences, 9, 1869-1888.

Pan C., Wang X., Liu L., Huang H., Wang D. (2017) Improvement to the Huff Curve for Design Storms and Urban Flooding Simulations in Guangzhou. China Water, 9, 411. doi:10.3390/w9060411.

Pilgrim D.H., Cordery I. (1975) Rainfall temporal patterns for design floods. Journal of the Hydraulics Division, 101, 81-95.

Raso J., Malgrat P., Castillo F. (1995) Improvements in the selection of design storms for the New Master Drainage Plan of Barcelona. Water Science and Technology, 32, 217-224.

Redaño A., Lorente J., Vázquez R. (1986) Climatología de las intensidades extremas de lluvia en Barcelona. Revista de Geofísica, 42, 193-198.

Rodríguez R., Navarro X., Casas MC., Ribalaygua J., Russo B., Pouget L., Redaño A. (2014) Influence of climate change on IDF curves for the metropolitan area of Barcelona (Spain). International Journal of Climatology 34, 643–654. doi.org/10.1002/joc.3712.

Schmid P.E., Niyogi D. (2013) Impact of city size on precipitation-modifying potential, Geophysical Research Letters, 40, 5263–5267. doi:10.1002/grl.50656.

Simonovic S.P., Schardong A., Sandink D., Srivastav R. (2016) A web-based tool for the development of Intensity Duration Frequency curves under changing climate. Environmental Modelling & Software, 81, 136-153.

Terranova O.G., Laquinta P. (2011) Temporal properties of rainfall events in Calabria (southern Italy). Natural Hazards and Earth System Sciences, 11, 751–757.

Terranova O.G., Gariano S.L. (2014) Rainstorms able to induce flash floods in a Mediterranean-climate region (Calabria, southern Italy). Natural Hazards and Earth System Sciences, 14, 2423–2434. doi:10.5194/nhess-14-2423-2014.

Willems P. (2013) Revision of urban drainage design rules after assessment of climate change impacts on precipitation extremes at Uccle, Belgium. Journal of Hydrology, 496, 166-177. doi.org/10.1016/j.jhydrol .2013.05.037.

Wright D.B., Smith J.A., Villarini G., Baeck M.L. (2012) Hydroclimatology of flash flooding in Atlanta. Water Resources Research, 48, W04524. doi:10.1029/2011WR011371.

Živković, M. (1995) Hierarchical clustering of atmospheric soundings. International Journal of Climatology, 15, 1099-1114. doi.org /10.1002/ joc.337 0151004.

Gauge	<R>	σ(R)	<L>	σ(L)	<I_{max}>	σ(I_{max})	I_M	Date(I_M)	R(I_M)	Ratio
1	45.0	21.8	446.8	324.3	4.7	2.6	10.0	09/07/2005	34.5	29.0
2	45.4	23.1	435.6	340.4	5.0	2.7	12.4	09/14/1999	60.7	20.0
3	51.1	20.7	568.9	394.2	4.2	2.6	9.0	09/14/1999	51.0	19.6
4	57.7	27.8	516.8	293.7	6.1	3.0	12.3	07/15/2001	66.7	18.4
5	47.6	23.3	448.2	318.9	5.6	3.3	15.5	09/14/1999	67.4	23.0
6	48.1	18.9	461.9	343.4	5.2	3.6	19.6	09/21/1995	91.9	21.3
7	43.9	22.1	416.5	334.2	5.9	3.1	12.4	09/14/1999	56.8	21.8
8	43.6	18.7	477.2	350.7	4.9	2.6	10.2	08/02/2005	30.9	33.0
9	51.7	21.4	516.8	342.8	4.8	2.6	11.4	09/14/1999	46.4	24.6
10	45.6	21.7	440.8	350.5	6.0	3.4	13.9	08/26/2002	40.5	34.3
11	55.5	23.3	463.3	328.5	6.5	3.4	14.0	09/14/1999	58.2	24.0
12	44.3	24.6	339.2	239.7	5.9	2.5	12.0	10/17/2008	28.3	42.4
13	53.4	27.1	581.8	427.3	4.7	2.6	10.1	10/17/1999	21.4	47.2
14	51.7	30.4	497.3	312.5	5.5	2.9	12.3	09/14/1999	51.0	24.1
15	43.7	20.7	455.0	325.2	5.4	2.8	12.3	09/14/1999	53.9	23.0
16	44.6	15.1	427.1	337.9	5.4	2.9	11.0	10/23/1997	32.6	33.7
17	54.2	25.2	448.7	340.2	5.8	3.1	11.7	11/17/1996	29.0	40.3
18	51.4	27.4	460.4	326.4	5.6	3.2	13.0	09/14/1999	51.0	25.5
19	45.3	19.5	467.8	319.0	4.9	2.9	10.5	10/05/1998	28.4	37.0
20	46.4	25.4	424.1	324.1	6.4	2.9	12.8	09/14/1999	47.2	27.1
21	45.4	23.2	408.1	291.4	5.3	2.5	9.9	10/17/1999	25.8	38.4
22	53.7	29.5	418.1	347.9	6.0	2.6	11.5	09/14/1999	48.6	23.7
23	56.8	24.5	514.6	412.6	5.4	3.5	11.3	08/24/1995	94.2	12.0

Table 1. Preliminary statistics of heavy rain records for every gauge: average, <**R**> and standard deviation, σ(**R**), given in mm, of rain amounts **R**, average, <**L**> and standard deviation, σ(**L**), given in min, of episodes length **L**, average, <$\mathbf{I_{max}}$>, and standard deviation, σ($\mathbf{I_{max}}$), of maximum 5-min rain amounts, $\mathbf{I_{max}}$, given in mm/5-min, the highest 5-min rain amount recorded at every gauge, $\mathbf{I_M}$, the date (month/day/year) for which this highest intensity is detected, **Date($\mathbf{I_M}$)**, and the rain amount, **R($\mathbf{I_M}$)**, for the record with this maximum intensity. **Ratio**, in percentage, is computed as the quotient between $\mathbf{I_M}$ and **R($\mathbf{I_M}$)**.

09/21/1995			09/14/1999			08/26/2002		
Gauge	**I_{max} (mm/5-min)**	**R (mm)**	**Gauge**	**I_{max} (mm/5-min)**	**R (mm)**	**Gauge**	**I_{max} (mm/5-min)**	**R (mm)**
1	7.2	36.7	1	7.8	50.3	1	0.6	2.9
2	1.8	12.7	2	12.4	60.7	2	6.1	26.4
3	8.2	35.1	3	9.0	43.1	3	3.5	14.3
6	19.6	91.9	4	2.4	10.0	5	3.7	17.1
7	4.7	22.8	5	15.5	67.4	6	2.3	9.3
8	6.5	30.5	6	5.7	26.0	7	8.9	27.0
9	4.4	39.4	7	12.4	56.8	8	0.8	6.4
10	3.0	22.8	8	9.6	33.4	9	0.9	6.6
11	9.6	55.1	9	11.4	46.4	10	13.9	40.5
13	2.4	23.0	10	11.8	52.7	11	5.0	15.9
15	0.6	6.1	11	14.0	58.2	12	4.1	13.7
16	4.2	23.0	14	12.3	51.0	15	6.8	21.1
18	8.3	40.4	15	12.3	53.9	16	8.8	31.0
19	7.8	35.4	16	8.3	56.2	17	1.8	10.8
20	3.2	18.4	17	10.9	59.9	20	0.6	4.0
22	8.5	89.2	18	13.0	51.0	21	0.2	0.9
23	10.0	55.4	19	7.8	60.0	22	1.0	5.0
240 min			20	12.8	47.2	**150 min**		
			21	8.5	38.4			
			22	11.5	48.6			
			23	11.2	43.3			
			115 min					

Table 2. Three examples of heavy rainfall episodes with some high intensities.

CLUSTER		Min(R) (mm)	Max(R) (mm)	<R> (mm)	I_{max} (mm/5-min)		$<I_{max}>$ (mm/5-min)	Min(L) (min)	Max(L) (min)
(a)	**(b)**				**Min**	**Max**			
1	225	25.1	136.5	51.6	0.5	15.5	4.9	70	1255
2	4	28.7	32.2	30.7	3.2	6.3	4.5	270	355
3	15	26.9	46.2	31.9	5.0	13.9	8.1	120	515
4	178	25.1	124.6	51.6	1.3	19.6	5.3	95	1490
5	59	25.3	56.4	35.4	1.9	11.9	7.1	100	650
6	4	29.0	42.6	34.2	7.0	9.6	8.2	240	270
7	5	25.3	38.3	33.1	4.6	10.7	8.4	170	285
8	2	26.8	31.3	29.1	3.3	9.2	6.3	130	185
9	4	25.7	37.1	31.5	6.1	11.6	8.4	155	155
10	3	27.9	34.7	30.7	8.7	12.0	10.5	410	410

Table 3. Minimum, **Min(R)**, maximum, **Max(R)**, average, **<R>**, rain amount, minimum, **Min(I_{max})**, maximum, **Max(I_{max})**, and average, **<I_{max}>**, 5-min rain amount and minimum, **Min(L)** and maximum, **Max(L)**, lengths. The clusters are identified by **(a)** their number~~,~~ and include **(b)** the number of records.

CLUSTER	φ
1	6.79
2	11.90
3	**17.99**
4	8.22
5	14.38
6	**19.45**
7	**20.93**
8	12.66
9	**17.88**
10	**24.98**

Table 4. Degree of irregularity, φ, with respect to uniform rainfall percentages along time deciles for every cluster. Bold types design the five highest irregularities.

Gauge	I_{max} (mm/5-min)	R (mm)	L (min)	Ratio (%)	R/L (mm/min)	DATE	CLUSTER
23	11.3	94.2	115	12.0	0.82	08/24/1995	1
6	19.6	91.9	240	21.3	0.38	09/21/1995	4
11	9.6	55.1	240	17.4	0.23	09/21/1995	4
22	8.5	89.2	240	9.5	0.37	09/21/1995	4
23	10.0	55.4	240	18.1	0.23	09/21/1995	1
2	12.4	60.7	115	20.4	0.53	09/14/1999	4
5	15.5	67.4	115	23.0	0.59	09/14/1999	1
7	12.4	56.8	115	21.8	0.49	09/14/1999	1
11	14.0	58.2	115	24.1	0.51	09/14/1999	1
16	8.3	56.2	115	14.8	0.49	09/14/1999	1
17	10.9	59.9	115	18.2	0.52	09/14/1999	1
4	12.3	66.7	220	18.4	0.30	07/15/2001	4
10	11.8	55.2	220	21.4	0.25	07/15/2001	4
3	8.5	74.5	300	11.4	0.25	07/31/2002	4
5	11.0	114.3	300	9.6	0.38	07/31/2002	4
11	7.9	72.7	300	10.9	0.24	07/31/2002	1
14	8.2	100.8	300	8.1	0.30	07/31/2002	4
16	8.9	81.0	300	11.0	0.27	07/31/2002	4
19	9.6	89.9	300	10.8	0.30	07/31/2002	4
20	8.0	91.7	300	8.7	0.31	07/31/2002	1
4	9.0	108.7	370	8.3	0.29	10/12/2005	1
14	9.0	136.5	370	6.6	0.37	10/12/2005	1
17	7.9	88.7	370	8.9	0.24	10/12/2005	1
20	8.8	122.5	370	7.2	0.33	10/12/2005	1
21	8.5	104.7	370	8.1	0.28	10/12/2005	1
22	10.2	124.3	370	8.2	0.36	10/12/2005	1
7	11.9	56.4	200	21.1	0.28	09/12/2006	5
15	10.4	55.5	200	18.7	0.28	09/12/2006	5
17	10.7	65.6	220	16.3	0.30	09/13/2006	4

Table 5. The highest heavy rainfall records: 29 records with $\mathbf{I_{max}}$ **, R** and **R/L** exceeding their respective 95% percentile of heavy rain episodes, together to their dates (month/day/year) and the number of cluster.

List of Figures

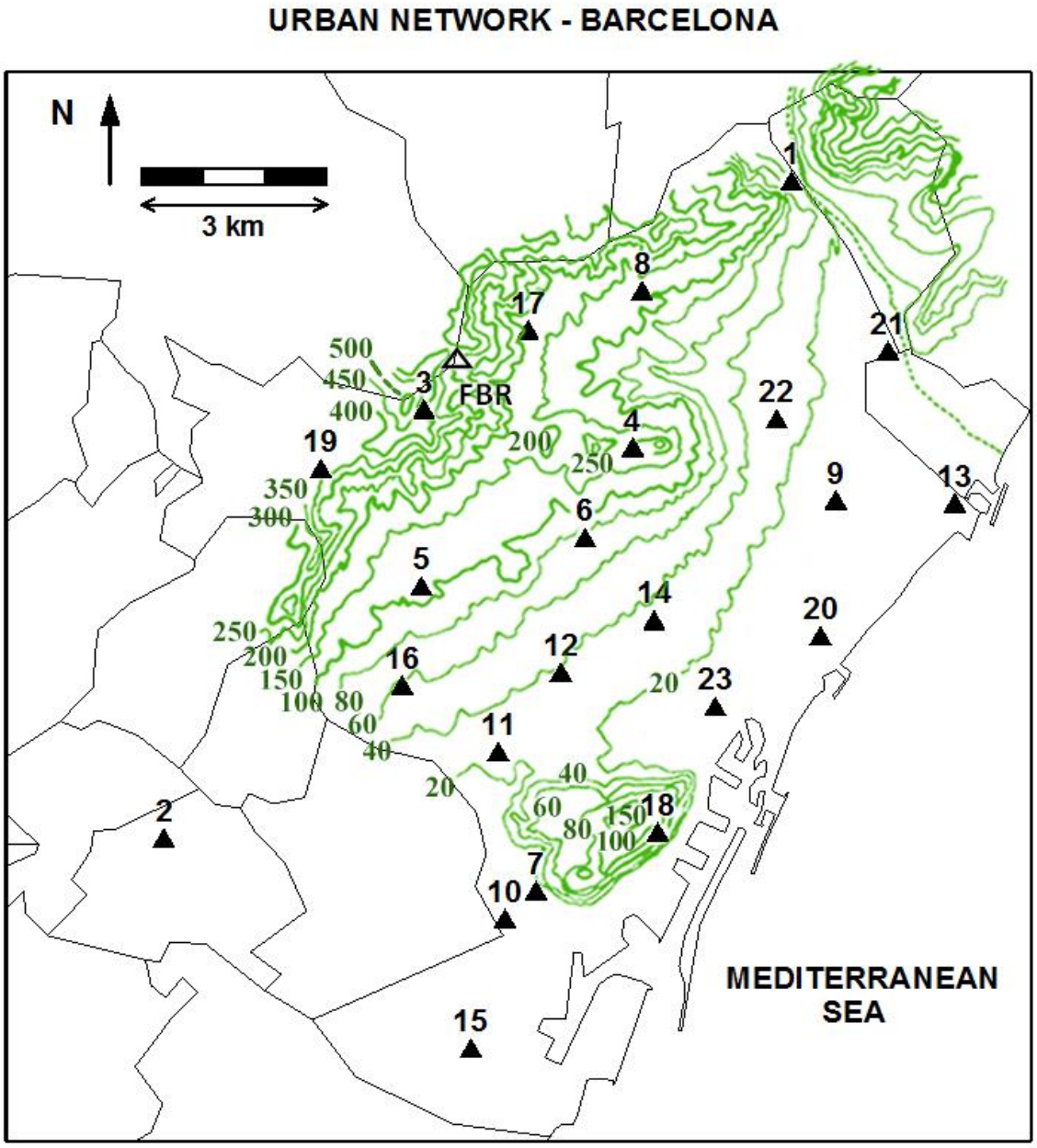
URBAN NETWORK - BARCELONA
N
3 km
FBR
MEDITERRANEAN SEA
1
2
3
4
5
6
7
8
9
10
11
12
13
14
15
16
17
18
19
20
21
22
23
500
450
400
350
300
250
200
150
100
80
60
40
20

Figure 1

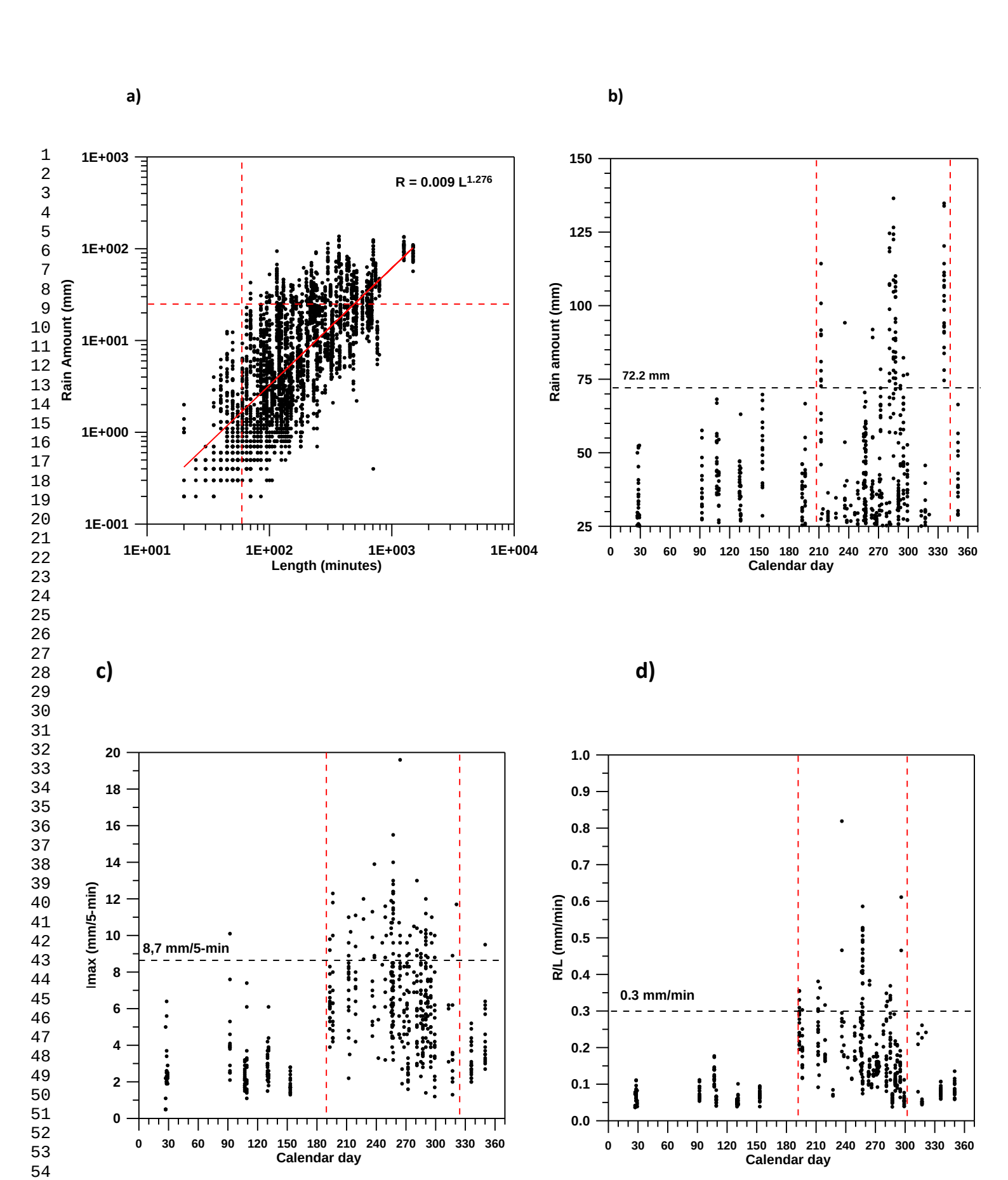
a)
b)
c)
d)
R = 0.009 L^1.276
Rain Amount (mm)
Length (minutes)
1E+001
1E+002
1E+003
1E+004
1E-001
1E+000
1E+001
1E+002
1E+003
Rain amount (mm)
72.2 mm
Calendar day
Imax (mm/5-min)
8,7 mm/5-min
R/L (mm/min)
0.3 mm/min

Figure 2

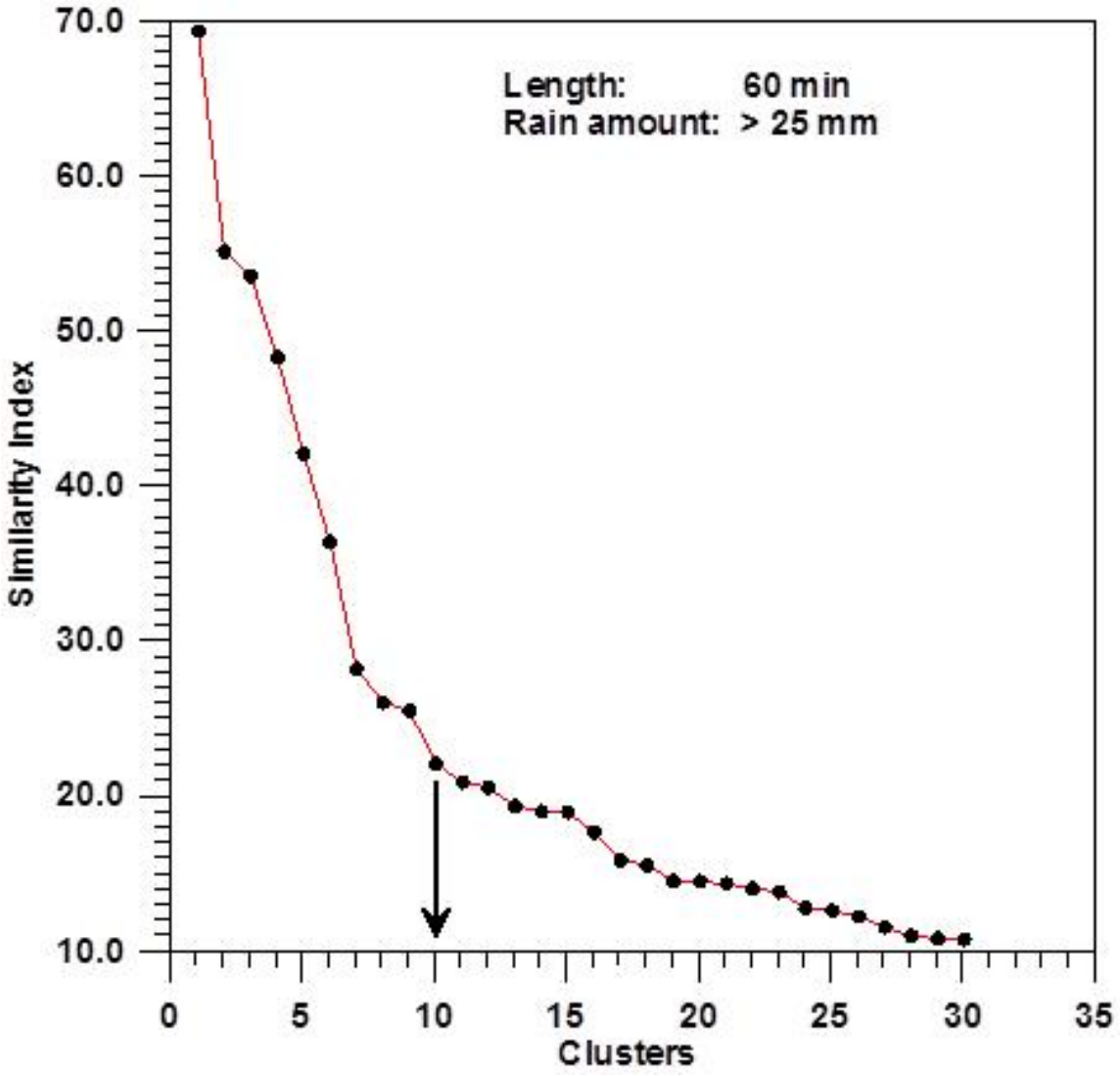
Length: 60 min
Rain amount: > 25 mm
Similarity Index
70.0
60.0
50.0
40.0
30.0
20.0
10.0
0
5
10
15
20
25
30
35
Clusters

Figure 3

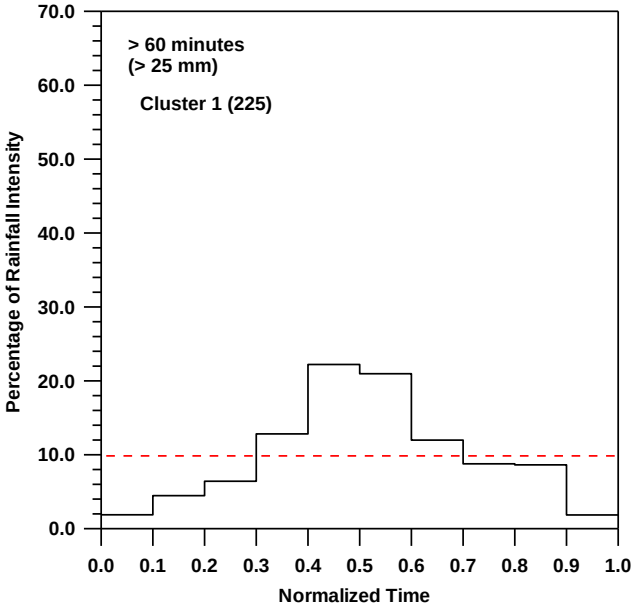
> 60 minutes
(> 25 mm)
Cluster 1 (225)
Percentage of Rainfall Intensity
Normalized Time

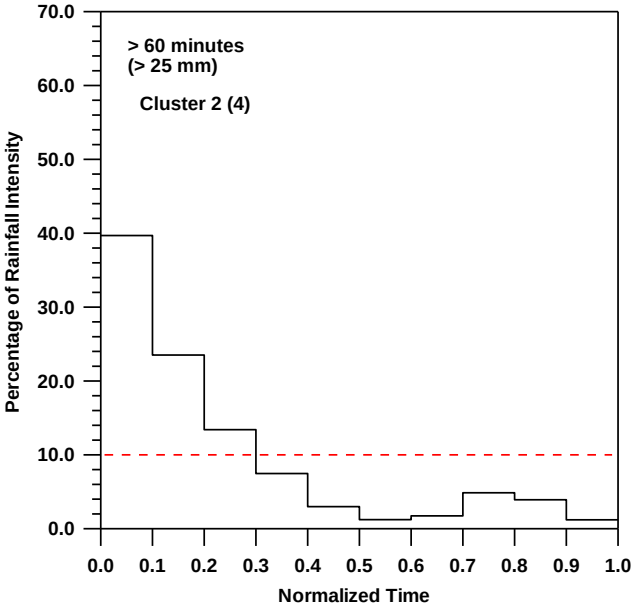
> 60 minutes
(> 25 mm)
Cluster 2 (4)
Percentage of Rainfall Intensity
Normalized Time

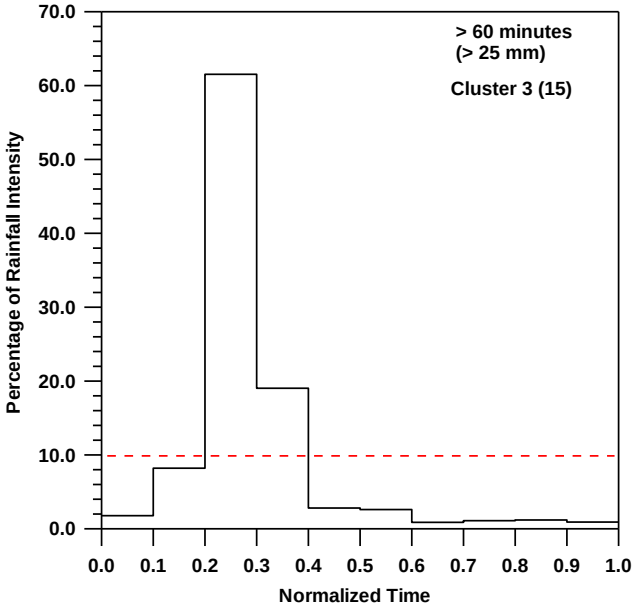
> 60 minutes
(> 25 mm)
Cluster 3 (15)
Percentage of Rainfall Intensity
Normalized Time

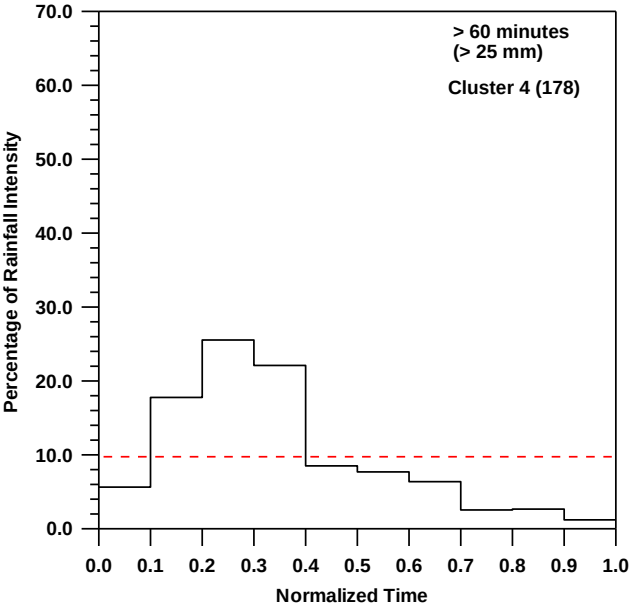
> 60 minutes
(> 25 mm)
Cluster 4 (178)
Percentage of Rainfall Intensity
Normalized Time

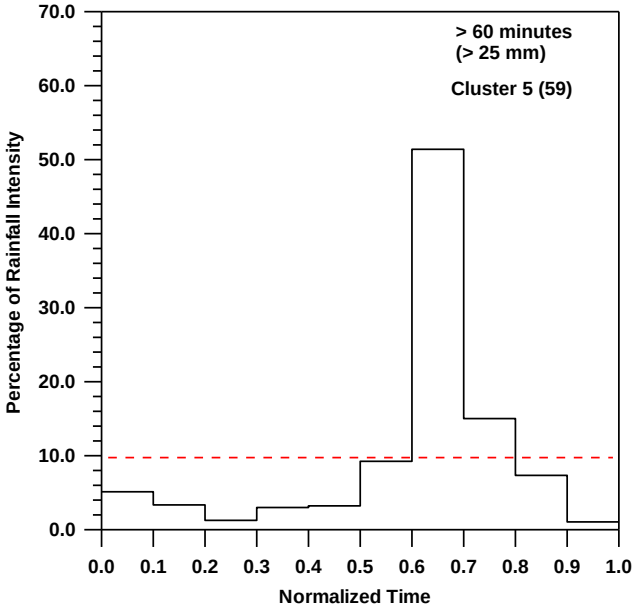
> 60 minutes
(> 25 mm)
Cluster 5 (59)
Percentage of Rainfall Intensity
Normalized Time

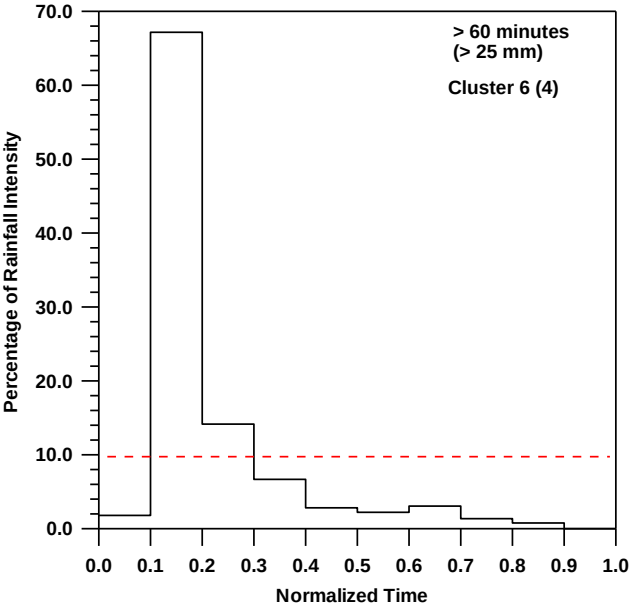
> 60 minutes
(> 25 mm)
Cluster 6 (4)
Percentage of Rainfall Intensity
Normalized Time

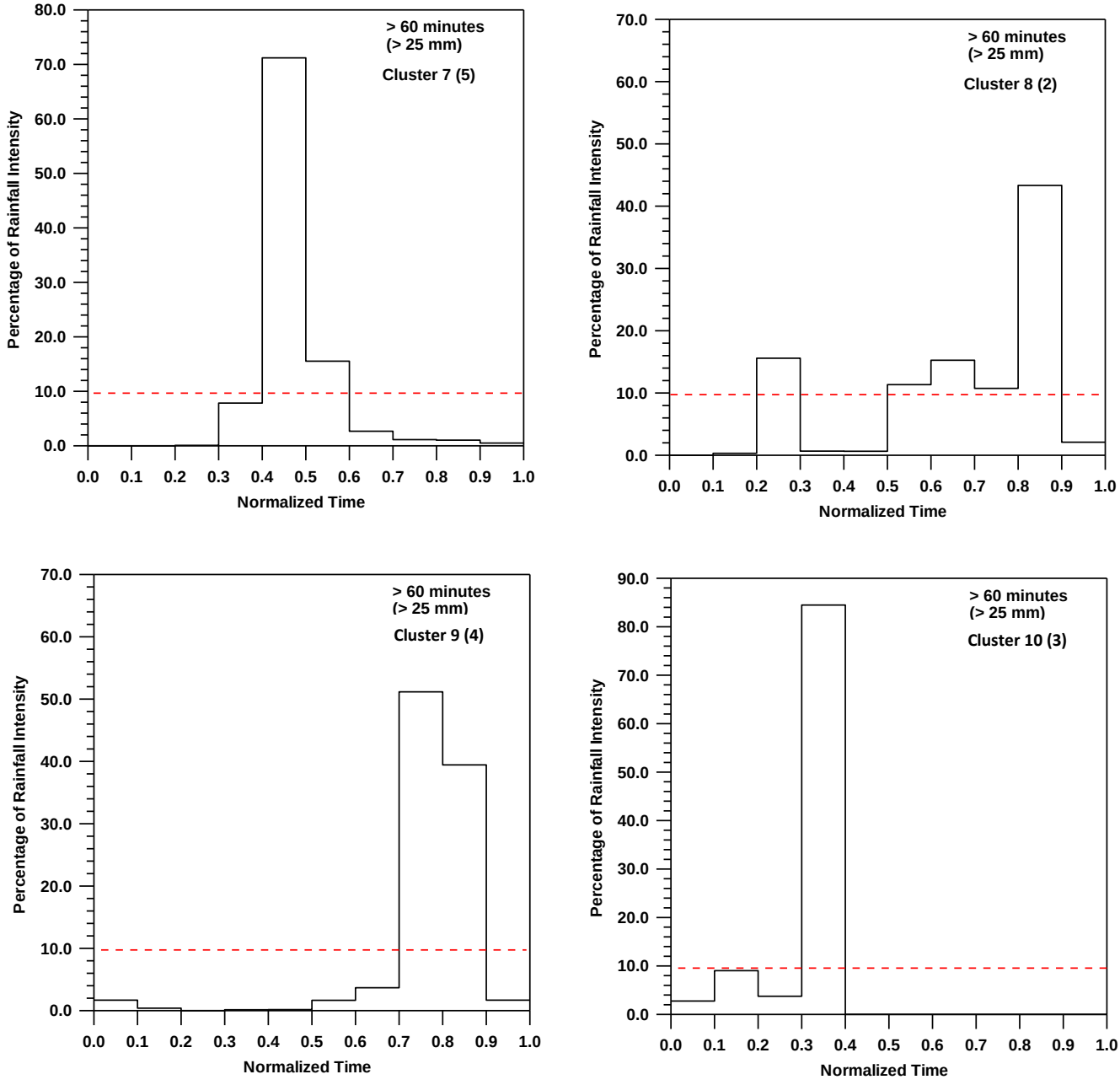
> 60 minutes
(> 25 mm)
Cluster 7 (5)
Cluster 8 (2)
Cluster 9 (4)
Cluster 10 (3)
Percentage of Rainfall Intensity
Normalized Time

Figure 4

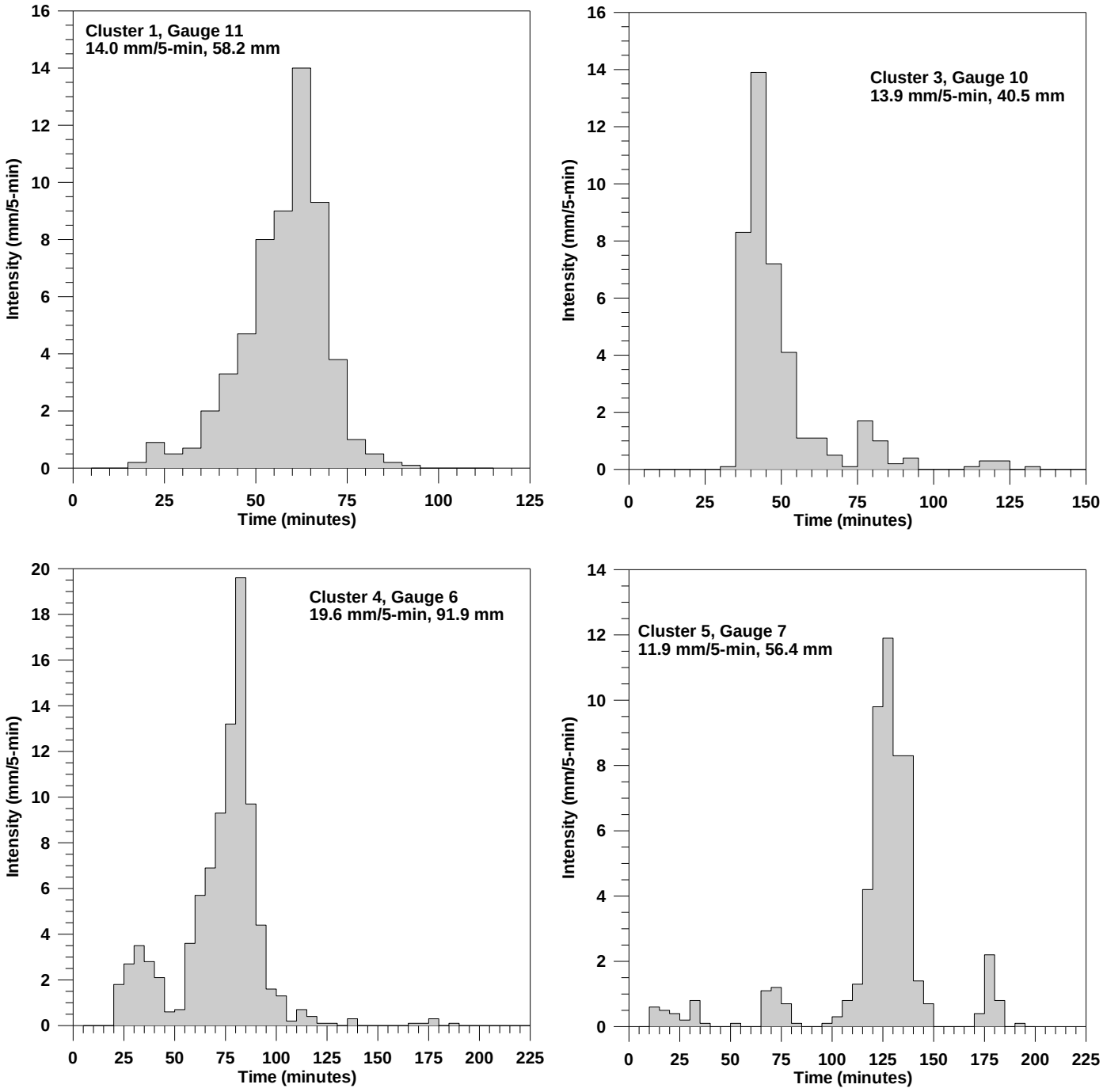
Cluster 1, Gauge 11
14.0 mm/5-min, 58.2 mm
Cluster 3, Gauge 10
13.9 mm/5-min, 40.5 mm
Cluster 4, Gauge 6
19.6 mm/5-min, 91.9 mm
Cluster 5, Gauge 7
11.9 mm/5-min, 56.4 mm
Intensity (mm/5-min)
Time (minutes)

Figure 5

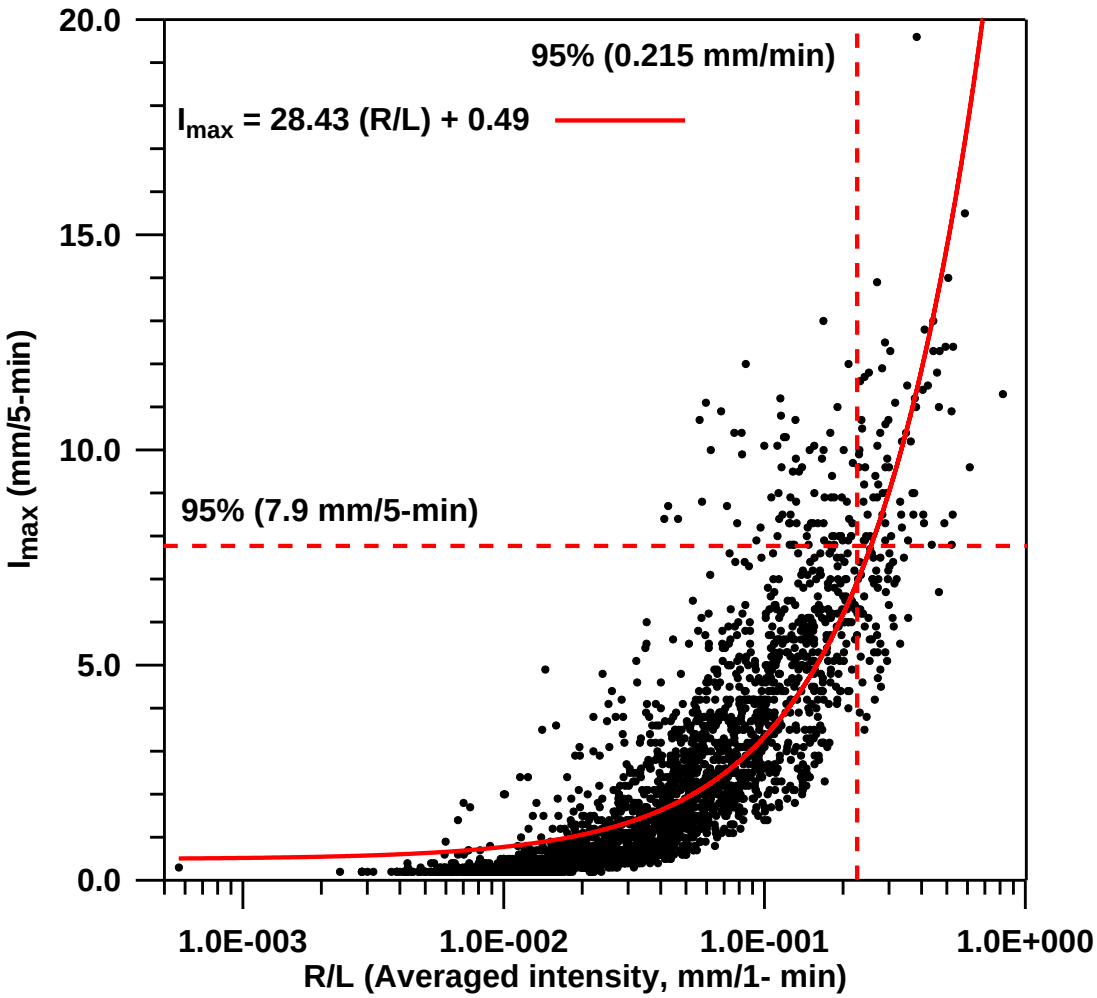
95% (0.215 mm/min)
I_{max} = 28.43 (R/L) + 0.49
95% (7.9 mm/5-min)
I_{max} (mm/5-min)
20.0
15.0
10.0
5.0
0.0
1.0E-003
1.0E-002
1.0E-001
1.0E+000
R/L (Averaged intensity, mm/1- min)

Figure 6

Manuscript:

Characterization of standardized heavy rainfall profiles for Barcelona city: Clustering, rain amounts and intensity peaks (TAAC-D-18-00869)

Answer to the reviewers:

Reviewer # 1.

A previous question to be clarified is that the AL algorithm does not classify either records for rain gauges locations, but standardised heavy rainfall profiles (First paragraph of Conclusions). Consequently, it is not surprising to detect several records of a same rainfall episode assigned to different clusters. Because of the standardization, the clustering process becomes possible without disturbances generate by the wide ranges of lengths and rain amounts (first lines Section 3.1).

a) Some references to previous statistics on rain rate in Fabra Observatory have been removed, given that they are not essential for this manuscript. These statistics correspond to years before the recording period of the rain rate gauges network.

b) The advantages of applying the clustering process to standardised rainfall profiles is explained in Section 3.1. Extreme heavy rainfalls pertain only to profiles of clusters 1, 4 and 5. These extreme heavy rainfalls would be mostly related to copious amounts (clusters 1 and 4) with quite uniform rainfall percentages along time deciles. Nevertheless, only two records pertain to cluster 5 with a clear irregular profile.

c) The 10 clusters finally obtained are not subjective. In agreement with the evolution of the L_{ij} parameter (Figure 3), 10 clusters would be right. Alternatively, seven clusters might be also an acceptable structure. Nevertheless, the smooth L_{ij} increase from the initial structure with 30 clusters notably changes when the step from 10 to 9 clusters is tested. It is also worth of mention (Conclusions) that extreme heavy rainfalls pertain only to clusters 1, 4 (notably regular profiles) and 5 (notable intensity peak close to the end of the rain profile).

d) The main objective of this manuscript is not solving specific questions concerning urban flash flood prevention (sewerage design, runoff, imperviousness or topography), but classifying standardised heavy rainfall profiles in clusters. It has been found that the extreme heavy rainfalls are detected from the end of summer up to beginning of autumn. Synoptic maps at surface and 500 hPa strongly suggest that the mechanism of these flash floods would be convective phenomena accompanied by cold air masses in altitude and weak pressure gradients at the Mediterranean coast.

Reviewer # 2.

a) The Abstract has been rewritten in agreement with suggestions of the reviewer. The main objectives of the manuscript are: analyses of heavy rainfalls from measures of 5-min rain amounts in an urban area, to permit a better understanding of factors causing flash floods, ground erosion and runoff, as well as on the design of sewerage structures. Details concerning Barcelona pluviometric regime and expected synoptic situations generating extreme heavy rainfalls are given in section 4.2 of the manuscript.

b) Blocks of the manuscript have been reorganised as follows:
Introduction: Only minor changes have been introduced in this Section.
Database:
1) A first part (*2.1 Database Details*) is devoted to describe the characteristics of the pluviometric network. The way how to decide the requirements (1 h as minimum length and amounts above or equal to 25 mm)

for selecting the heavy rainfalls, based on reports of two public meteorological services (AEMET and SMC), has been rewritten for a better understanding of these length and amount thresholds.

2) The main characteristics (*2.2 Preliminary Statistics*) of the 499 heavy rainfall records pertaining to 67 rainfall episodes are summarised in this new Section of *Database* by describing a set of parameters (average and standard deviation of rain amounts, lengths and 5-min rain amounts, as well as the maximum 5-min rain amount) for every rain gauge.

Methodology:

The Average Linkage algorithm is briefly described (Section 3.2) and reasons why the different lengths of the 499 heavy rainfall records and the corresponding 5-min rain amounts are standardised are given in Section 3.1. Comments and descriptions of the main characteristics of the 499 heavy rainfall records have been moved to Section 2.2 (*Preliminary Statistics*).

Results:

A few changes and comments on Clustering of the Profiles (Section 4.1) and extreme heavy rainfalls (Section 4.2) have been added. Concretely, new paragraphs are now given taking into account that:

a) Extreme heavy rainfalls have been detected in August, September and beginning of October.

b) A high degree of irregularity factor φ does not necessarily imply a heavy rainfall episode.

c) The finally chosen eight extreme heavy rainfall episodes have generated flash floods, as both local newspapers and scientific papers confirm.

d) Emplacements of gauges with extreme heavy rainfalls are coincident with those where return period maps of previous analyses quantified 5-min intensities maxima.

e) The synoptic situations for the extreme heavy rainfalls are very similar: vicinity to a 500 hPa trough and weak pressure gradients at surface level, together to small eastern advections.

Conclusions:

This section has been rewritten summarising the main objectives and results of the study. By one hand results concerning the clusters obtained and their properties. On the other hand results corresponding to extreme heavy rainfalls and their relevance on studies concerning urban ground drainage and sewerage designs.

With respect to the period analysed (15 years), the authors recognize it as excessively short to obtain, for instance, values with 25 years of return period. However, the sample of 499 heavy rainfall records pertaining to 67 episodes should be representative enough, being possible to extract 29 extreme records.

Reviewer # 3.

1) Green and black lines in Figure 1 correspond to isohipses and municipality borders respectively (new foot note of Fig. 1).
2) The heavy rainfall patterns can be summarised (Sections 4.1 and 4.2 and Conclusions) as follows:
    a) Heavy rainfalls are all of them detected at the end of August, September and beginning of October, when convective phenomena and eastern advection are expected.
    b) Thresholds for amounts and maximum and average 5-min rain amounts generating extreme heavy rainfalls are determined by considering 95% percentiles of these rainfall parameters from the 499 5-min rain amount records.
    c) After revising synoptic maps, it is concluded that extreme heavy rainfalls have been generated by convective phenomena, with cold air masses at 500 hPa level and weak pressure gradients at surface level. It is relevant to observe that the forecasting of these episodes becomes difficult, because the vicinity of a trough at 500 hPa level does not always generate intense and copious rainfall.
    d) Extreme heavy rainfalls are heterogeneously spatial distributed in the urban area.

e) Emplacements of gauges with extreme heavy rainfalls are coincident with those where return period maps of previous analyses quantified 5-min intensities maxima.
f) This research on heavy rainfalls, as well as previous researches, would be a contribution to a better design of drainage and sewerage in Barcelona city.
g) The results obtained, combined with detailed knowledge of the imperviousness density and the topography of the urban area, should be of application to get a better rainfall water infiltration in the ground, then mitigating runoff and sometimes also preventing saturation of sewer network.
h) The mitigation of urban heat island phenomenon could not be discarded when a not negligible part of rain water was absorbed by a porous ground.

EDITOR.

1) Figure 7 has been removed given that it was not necessary.
2) Conclusions have been structured and rewritten according to TAAC rules.